Oxidation-Induced Stacking Fault and Fast Pulling in Czochralski-Grown Silicon Crystals

Hak-Do Yoo, Hyun Jung Oh and Jong Hoe Wang

R & D Center, LG Siltron Inc., Korea

December 4, 1999

OiSF

What is OiSF?

Oxidation **I**nduced **S**tacking **F**aults (OISF) are plane defects generated in the surface region of silicon wafers during thermal oxidation process at typical temperature range between 900 and 1200℃

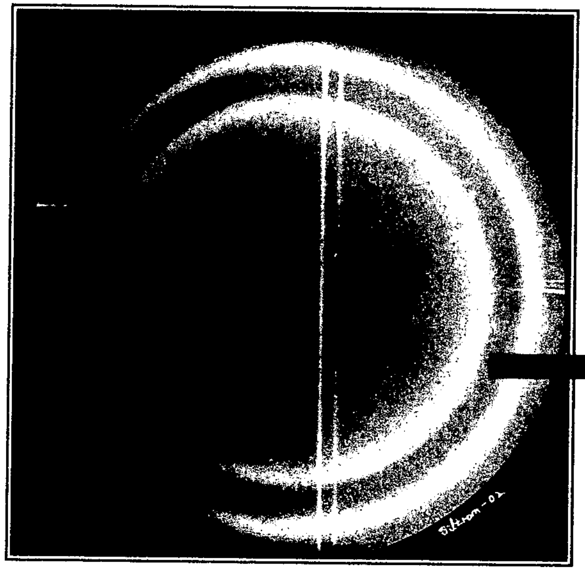

OISF-ring in a (100) silicon wafer. Revealed by Lang X-ray topography with Mo $K_{\alpha 1}$/g440 diffraction.

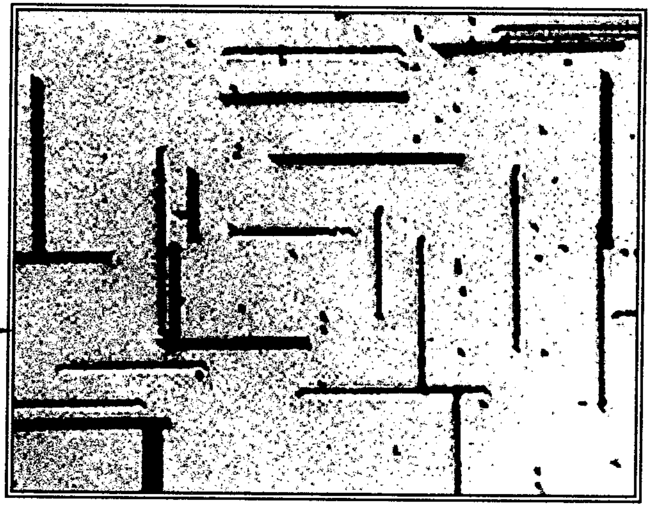

OISF generated on (100) wafer surface after Wright etching

OiSF

Oxygen-related Defects and Temperature Distribution

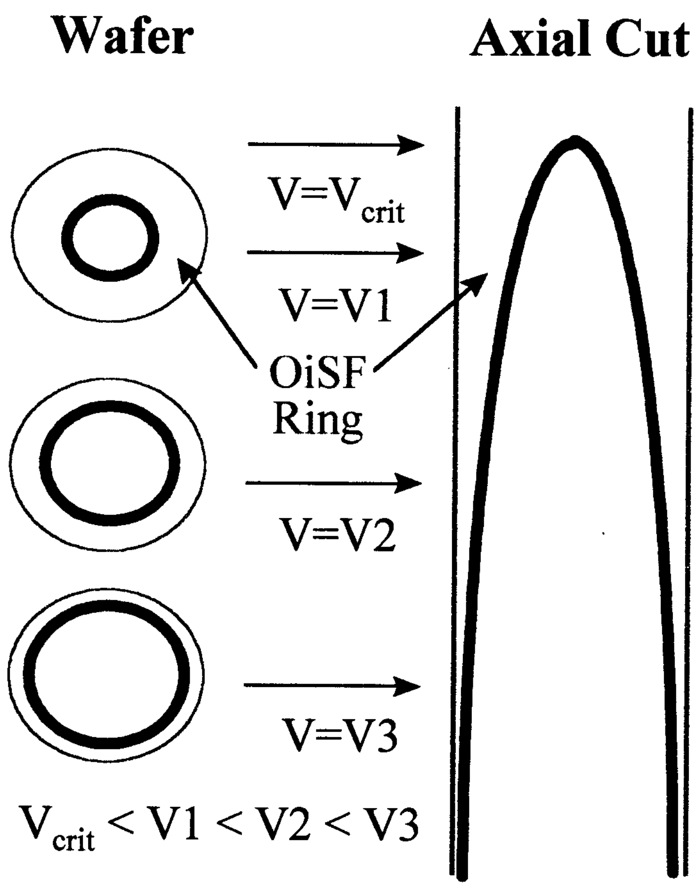

Wafer

Axial Cut

$V=V_{crit}$

V=V1

OiSF Ring

V=V2

V=V3

$V_{crit} < V1 < V2 < V3$

$V=v/G(r)$

STHAMAS 2DA

- In many materials processing technologies like casting and crystal growth, the process are controlled by heat transfer in complex geometry.
- The computer code STHAMAS is designed to be used as a tool for the analysis of heat transfer problems in crystal growth configurations.
- STHAMAS stands for

  Stress, Heat and mass Transfer Analysis using a Multigrid Accelerated Solver.
- STHAMAS 2DA consists of three program packages
  - GRIDE : Preprocessor written in C
  - STHAMAS : Main Processor written in FORTRAN 77
  - SHOW : Postprocessor written in C

  SUI (STHAMAS User Interface) :

  three modules are linked together by a graphical user interface

User Guide for STHAMAS 2DA (May, 1997) Erlangen, Germany

STHAMAS 2DA

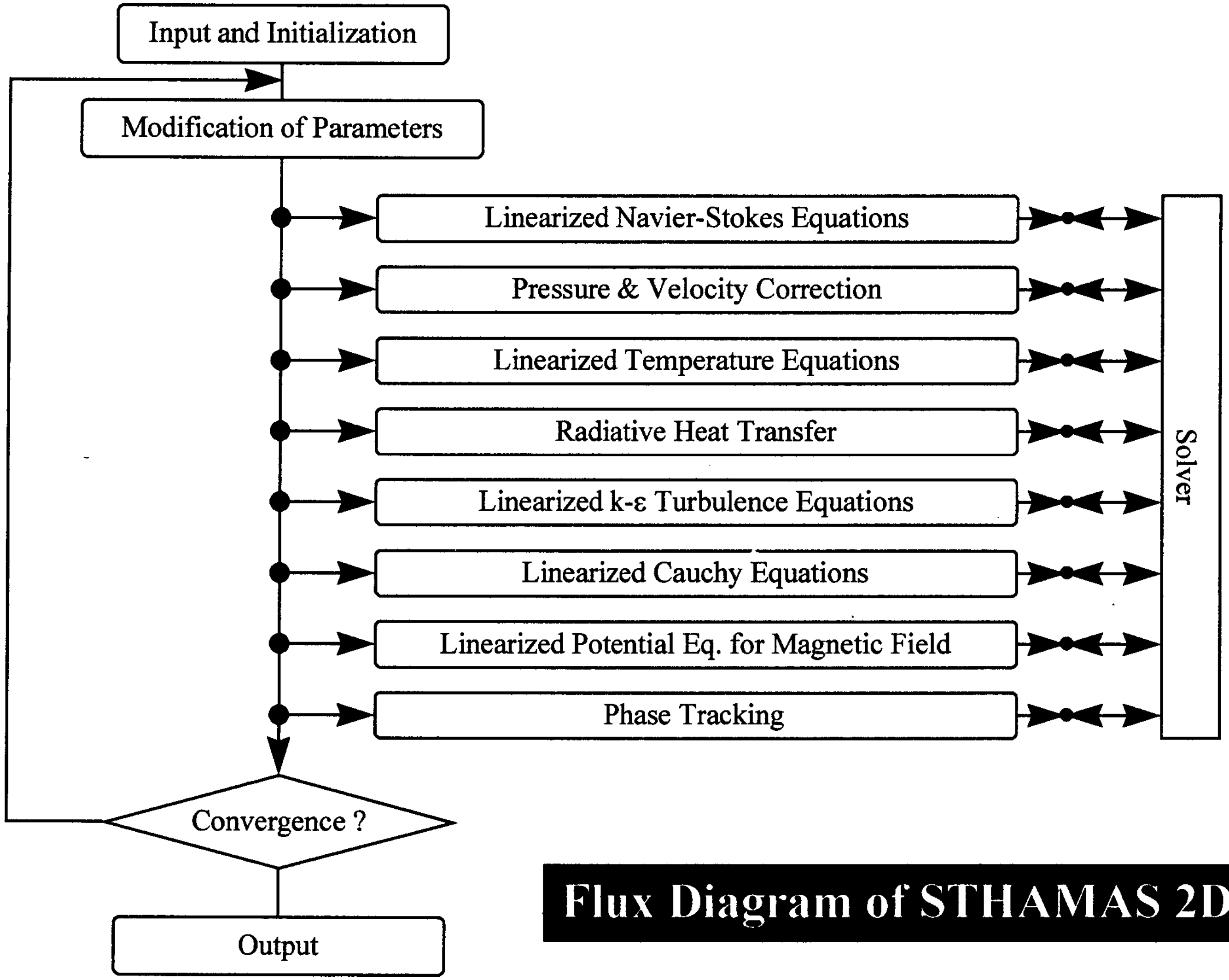

Input and Initialization

Modification of Parameters

Linearized Navier-Stokes Equations

Pressure & Velocity Correction

Linearized Temperature Equations

Radiative Heat Transfer

Linearized k-ε Turbulence Equations

Linearized Cauchy Equations

Linearized Potential Eq. for Magnetic Field

Phase Tracking

Solver

Convergence ?

Output

Flux Diagram of STHAMAS 2DA

STHAMAS 2DA

Comparison with Experiment

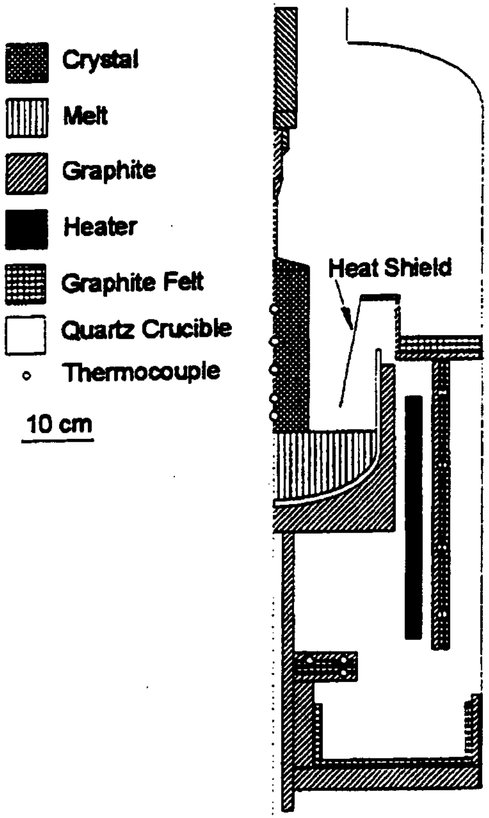

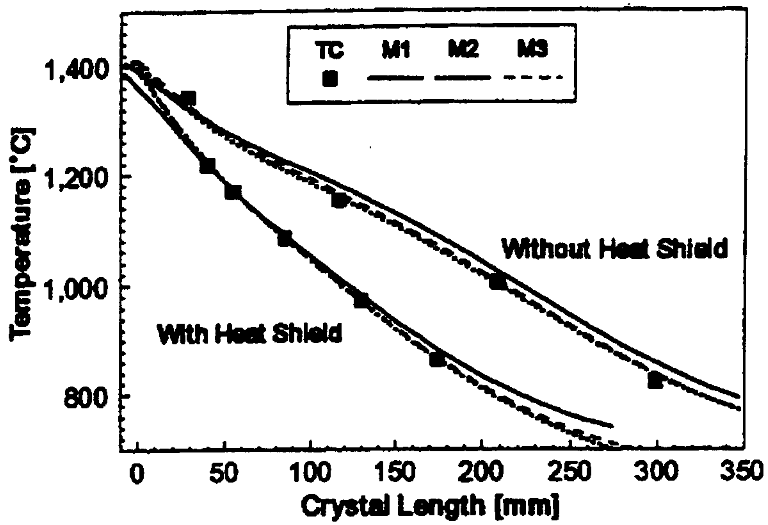

M1	Erlangen (STHAMAS 2DA)	FVM
M2	Catholique de Louvain (FEMAG)	FEM
M3	MIT (IHTCM)	FEM

E. Dornberger et al., Proceed. 2nd International Workshop for Modelling in Crystal Growth (1996) 45-47

Axial Temperature Distribution

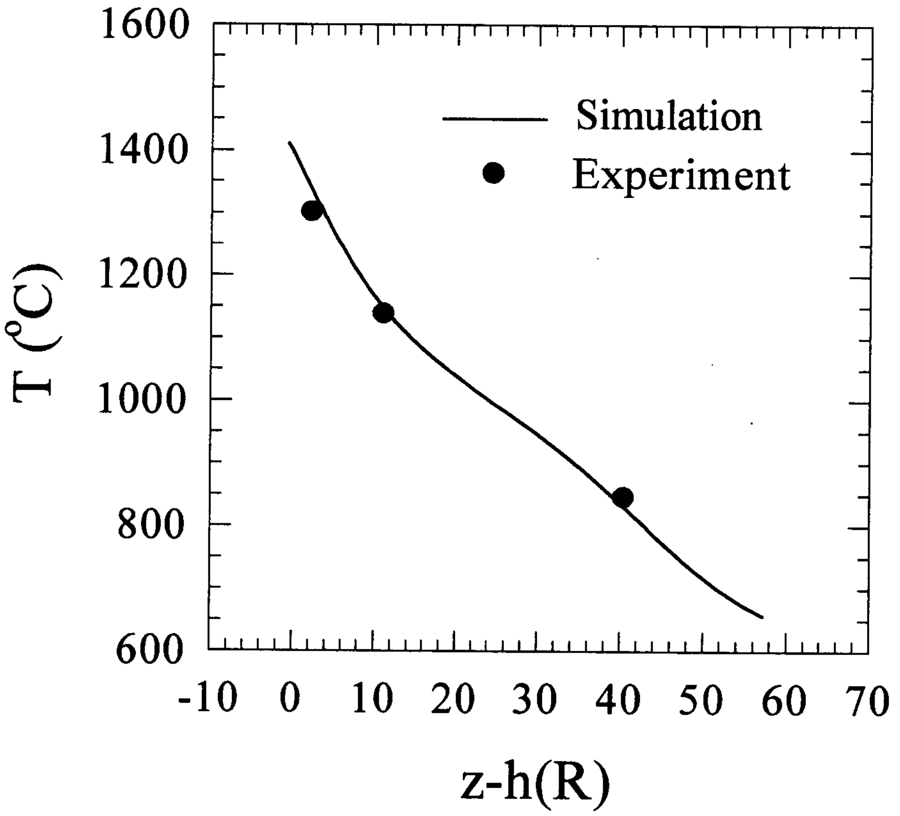

Mathematical Model

Governing Equations

$$\frac{DC_I}{Dt} = \nabla\cdot(-D_I\nabla C_I + \frac{C_I D_I H_I^f}{kT^2}\nabla T) + k_{IV}[C_I C_V - C_I^{eq} C_V^{eq}]$$

$$\frac{DC_V}{Dt} = \nabla\cdot(-D_V\nabla C_V + \frac{C_V D_V H_V^f}{kT^2}\nabla T) + k_{IV}[C_I C_V - C_I^{eq} C_V^{eq}]$$

k_{IV} : kinetic rate constant for the rate of vacancies and intersitials

C_I^{eq}, C_V^{eq} : Equilibrium concentrations of intersitials and vacancies

D_I, D_V : Diffusion coefficients for intersitials and vacancies

H_I^f, H_V^f : Enthalpies of formation of the point defects

k : Boltzman constant

Boundary Conditions

$C_j = C_j^{eq}(T_m)$ $j=I,V$ along the melt / crystal interface

$\mathbf{n}\cdot\mathbf{J}_j=0$ $j=I,V$ along the exposed crystal surface

$\mathbf{J}_j$: flux of the point defect j

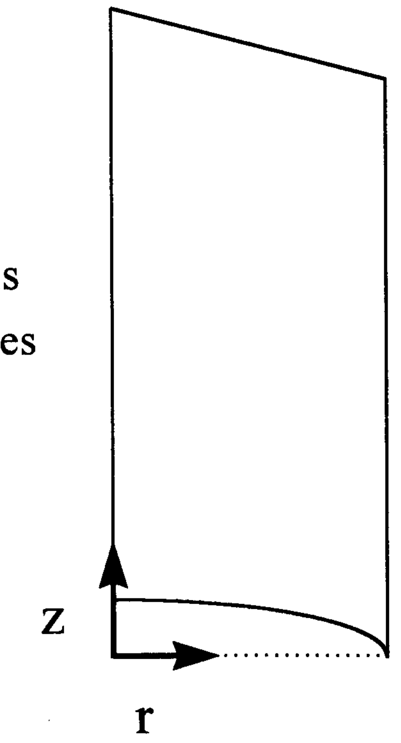

Schematics of Computational Domain

Thermophysical Properties of Point Defects

$$C_I^{eq} = 3.945 \times 10^{26} \exp(-\frac{3.943 \text{ eV}}{kT}) \ [\text{atoms} / \text{cm}^3]$$

$$D_I = 2.101 \times 10^{-1} \exp(-\frac{0.907 \text{ eV}}{kT}) \ [\text{cm}^2 / \text{sec}]$$

$$C_V^{eq} = 2.675 \times 10^{23} \exp(-\frac{2.848 \text{ eV}}{kT}) \ [\text{atoms} / \text{cm}^3]$$

$$D_V = 1.000 \times 10^{-4} \exp(-\frac{0.489 \text{ eV}}{kT}) \ [\text{cm}^2 / \text{sec}]$$

$$k_{IV} = \frac{4\pi a_r}{\Omega c_s}(D_I + D_V)\exp(-\frac{\Delta G_{IV}}{kT})$$

[R. A. Brown et al., *JCG* **137** (1994) 12-25]

$$\Delta H_{IV} = 3.173 \text{ eV}$$

$$\Delta S_{IV} = 15.0k$$

Comparison of Thermophysical Properties to Literature Estimates

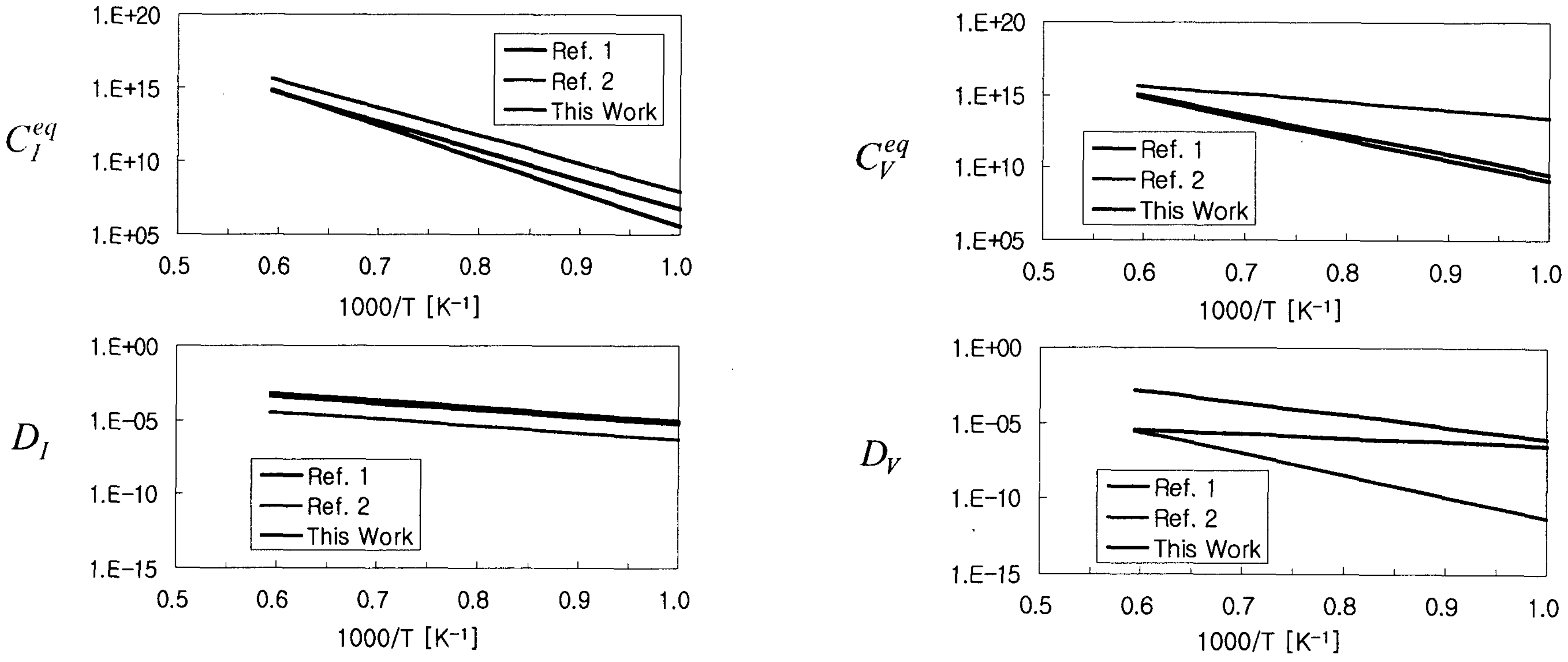

Ref. 1 : R. Habu and A. Tomiura, *Jpn. J. Appl. Phys.* **35** (1996) 1

Ref. 2 : H. Zimmermann and H. Ryssel, *J. Appl. Phys. A* **55** (1992) 121

Numerical Analysis

- Temperature Distribution : STHAMAS 2DA [Global Simulator]
- Discretization of Domain : Galerkin Finite Element Method
    - 9 node Lagrangian quadrilateral finite element
    - concentration : Biquadratic Lagrangian basis function
- Linearization : Newton-Raphson Method
    - Jacobian Matrix is obtained with closed form
- Numerical Integration : Gaussian Quadrature
    - 9-point Gaussian quadrature for volume integral
    - 3-point Gaussian quadrature for surface integral
- Solution for linear algebraic equations : Frontal Solver
    - efficient computation
    - minimization of core memory

Point Defect Dynamics

OiSF Ring Position (HZ1)

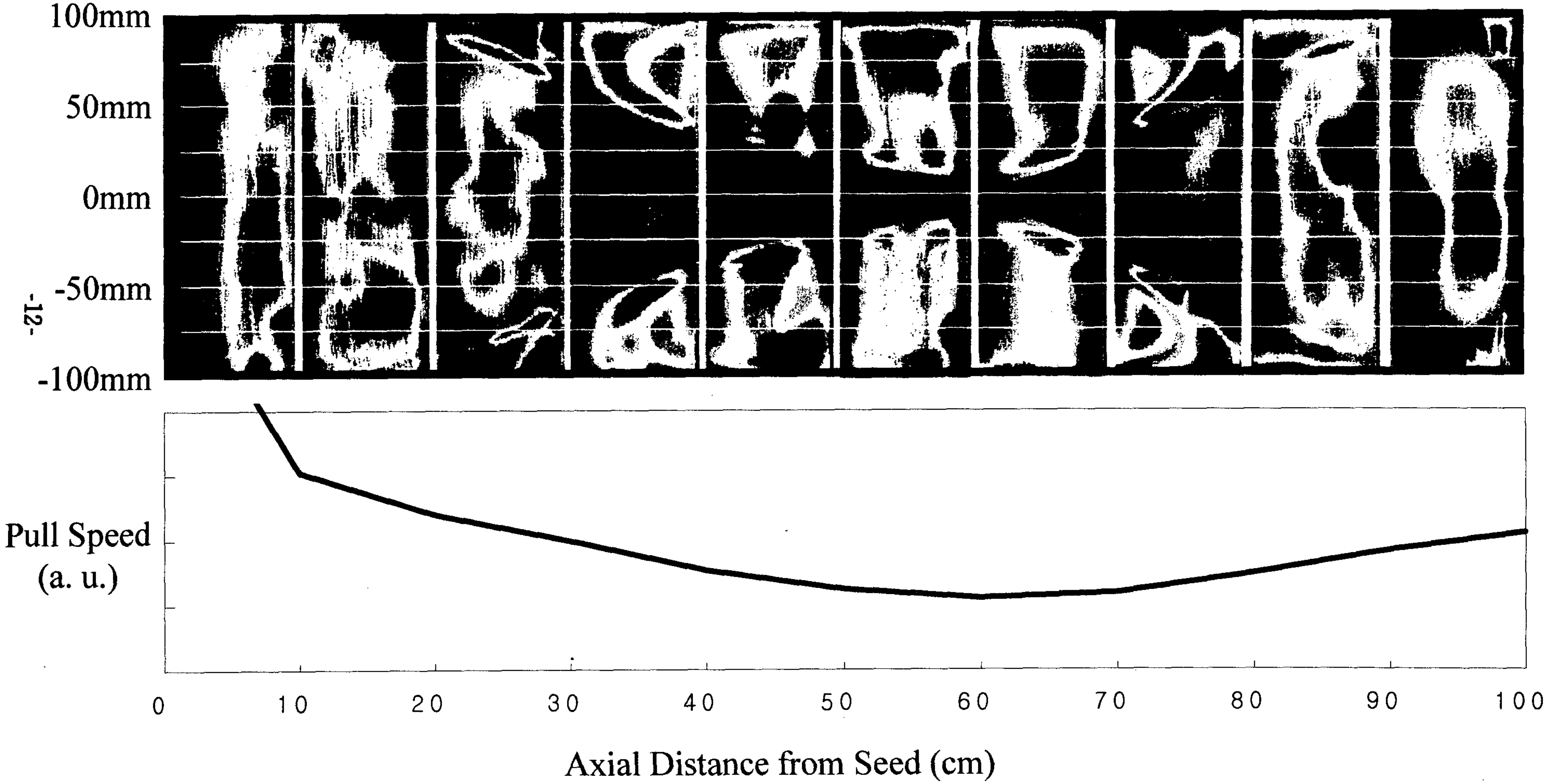

Point Defect Dynamics

OiSF Ring Position (HZ2)

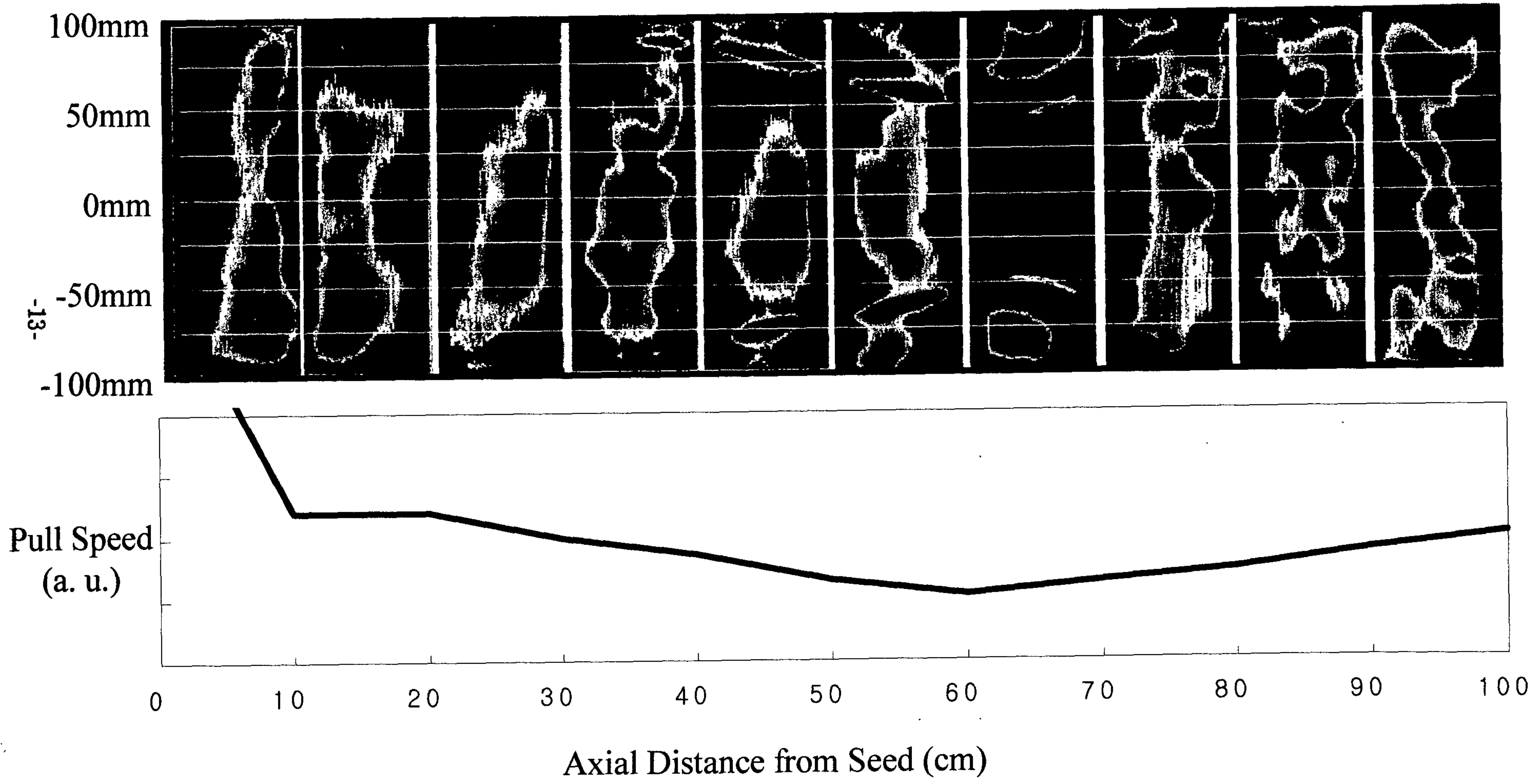

제 16차 KACG 가을학술발표회 LG Siltron R & D Center

Point Defect Dynamics

Temperature Distribution (HZ2)

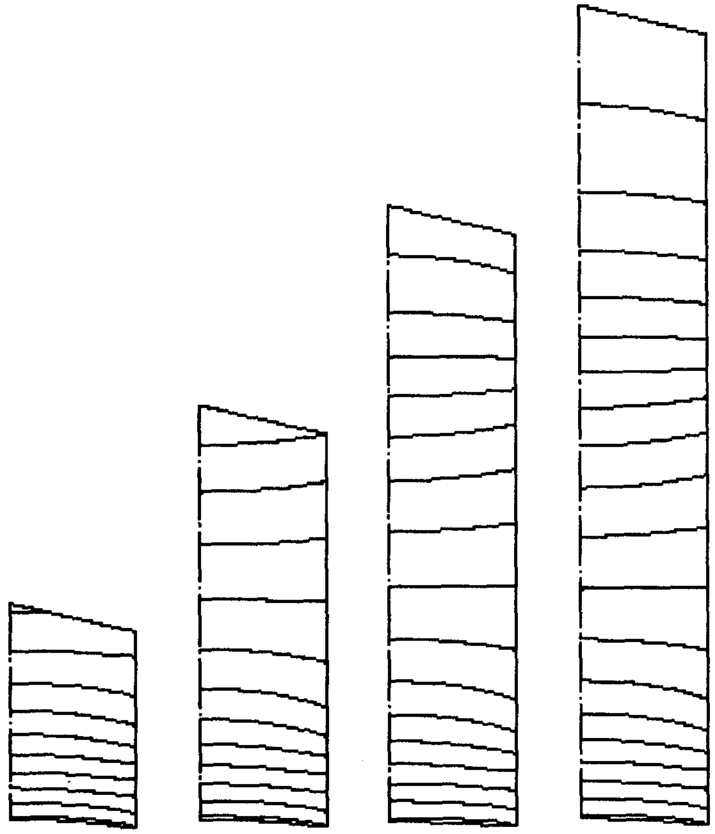

(a) 20 cm (b) 40 cm (c) 60 cm (d) 80 cm

Relative Supersaturation Distribution (HZ2)

$$\Delta = C_I - C_V$$

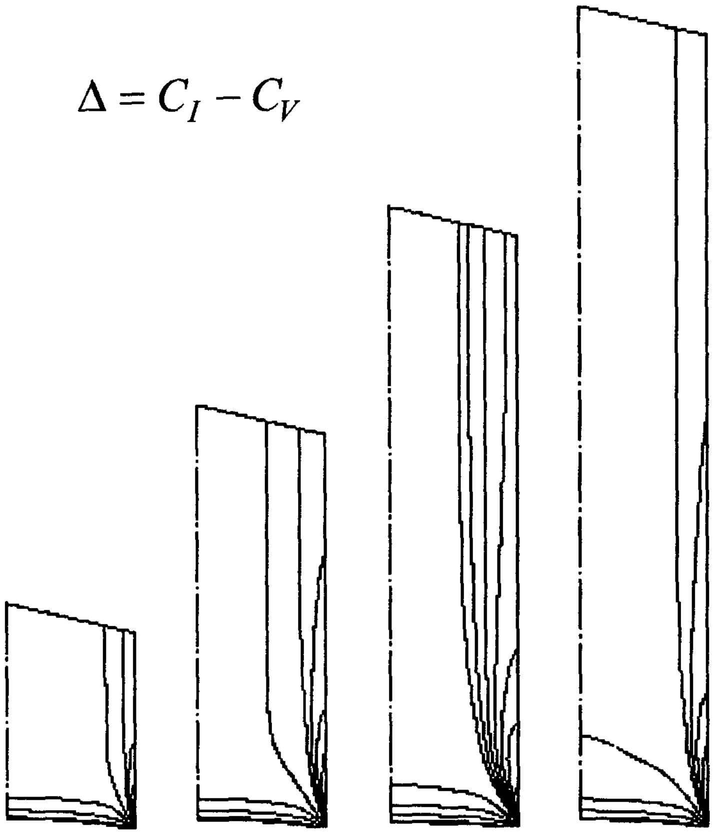

(a) 20 cm (b) 40 cm (c) 60 cm (d) 80 cm

Point Defect Dynamics

Comparison of Simulation and Experiments for OiSF Ring Dynamics

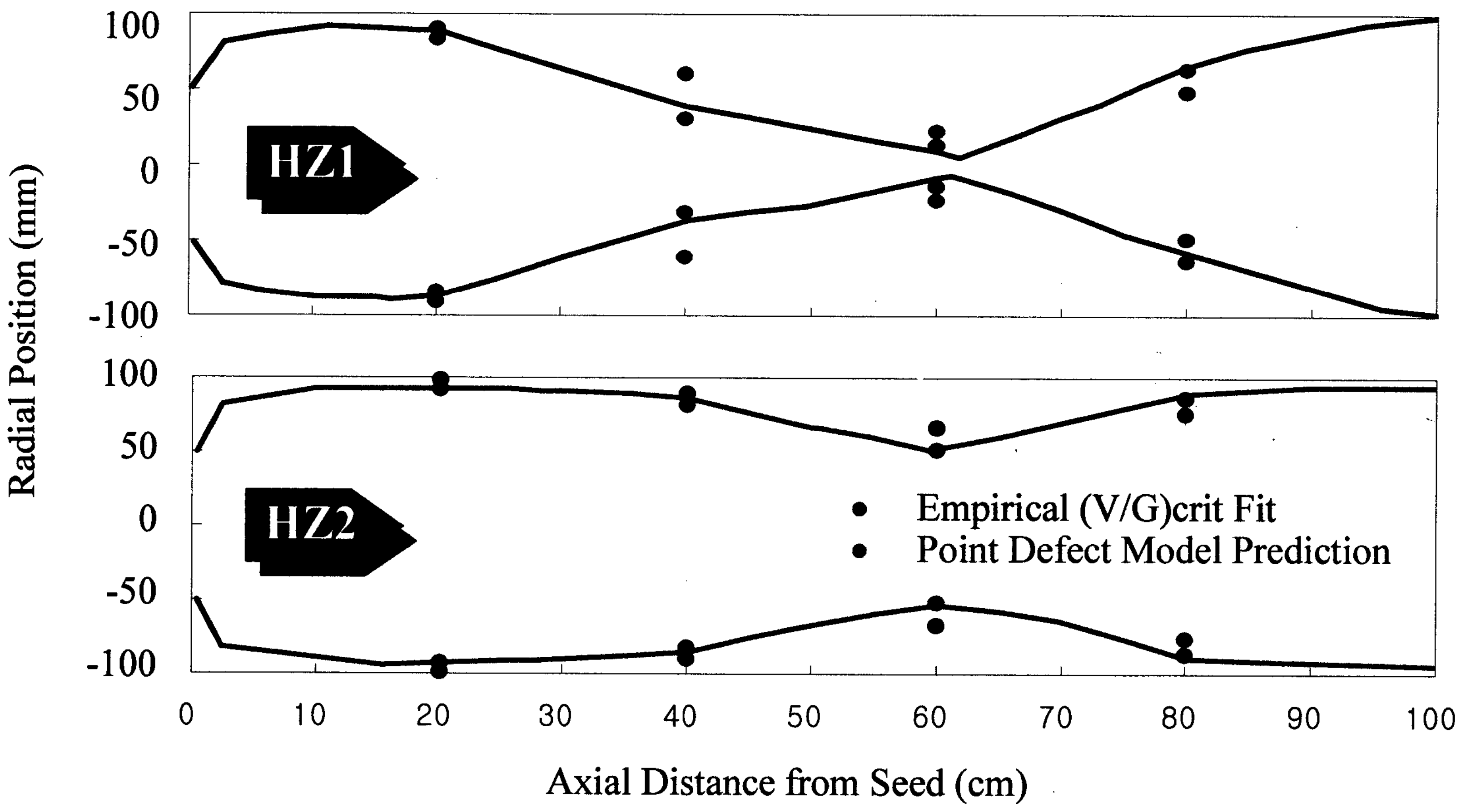

Conclusions (I)

- The continuum model of point defect dynamics is established by estimating expressions for equilibrium, transport and kinetic parameters.
- The numerical computations give a detailed picture of the development of the self-interstitial and vacancy distributions in a crystal during Czochralski crystal growth.
- The predictions of the numerical analysis for transition from vacancy to self-interstitial dominated regions are in good agreement with experiments when correlated with the location of the OiSF ring.
- This work will give the basis for direct comparison between simulation and the observation of microdefect distributions in Czochralski-grown silicon wafers.

Fast Pulling

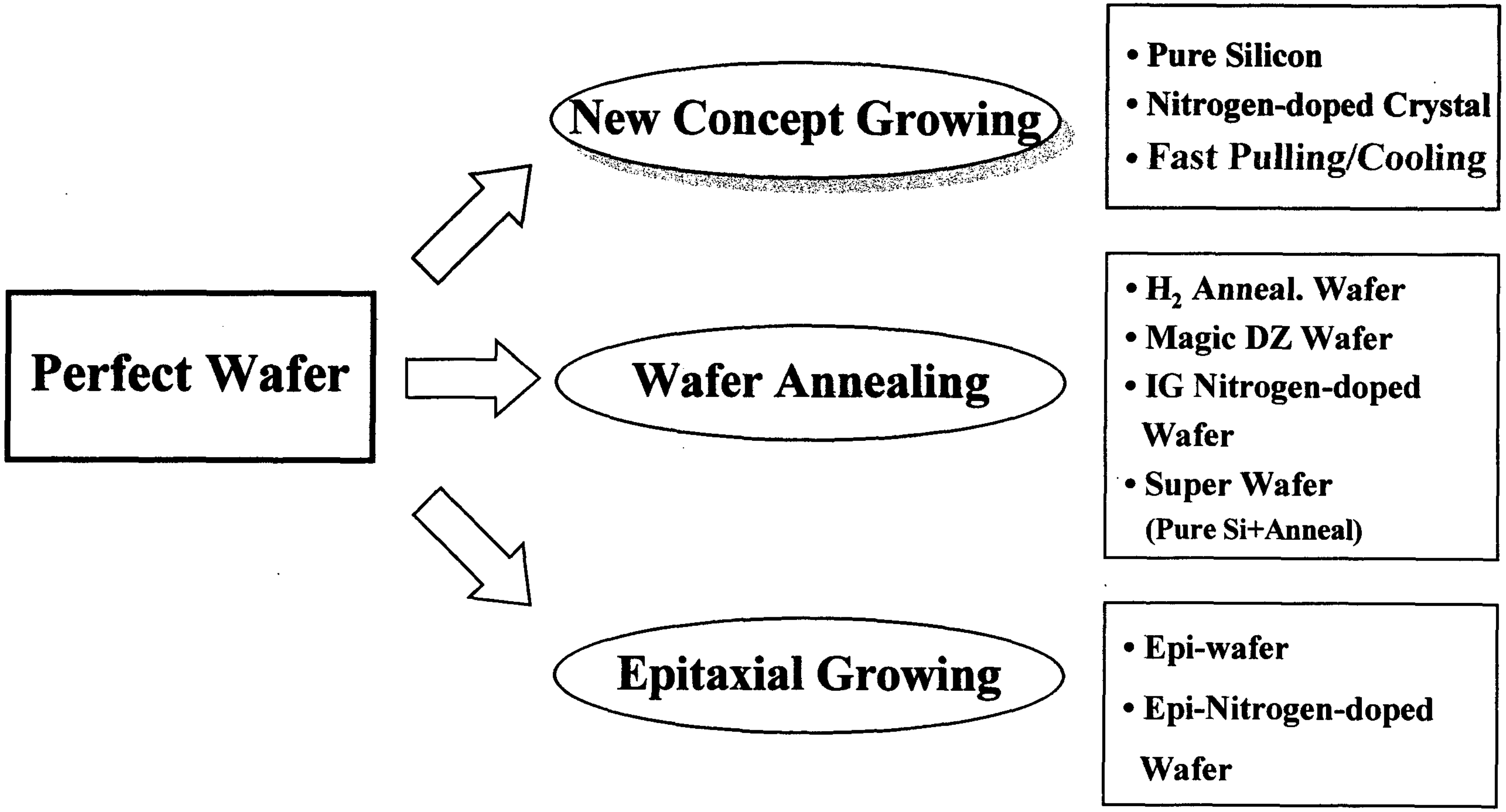

Perfect Wafer

New Concept Growing

- Pure Silicon
- Nitrogen-doped Crystal
- Fast Pulling/Cooling

Wafer Annealing

- H_2 Anneal. Wafer
- Magic DZ Wafer
- IG Nitrogen-doped Wafer
- Super Wafer (Pure Si+Anneal)

Epitaxial Growing

- Epi-wafer
- Epi-Nitrogen-doped Wafer

Fast Pulling

Behavior of Grown-in Defect during Crystal Growth

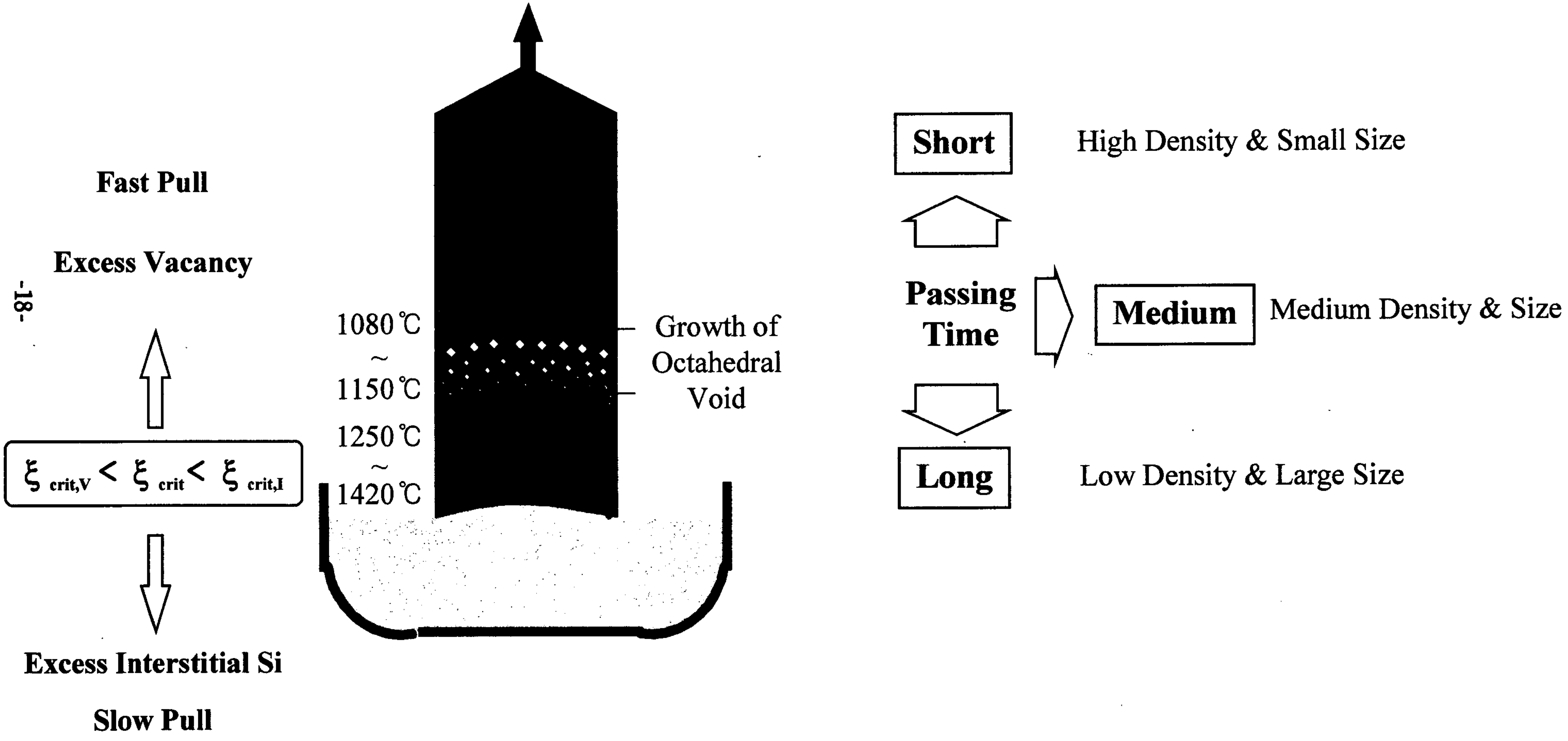

제 16차 KACG 가을학술발표회 LG Siltron R & D Center

Fast Pulling

Uniformity of Grown-in Defect by Pull speed

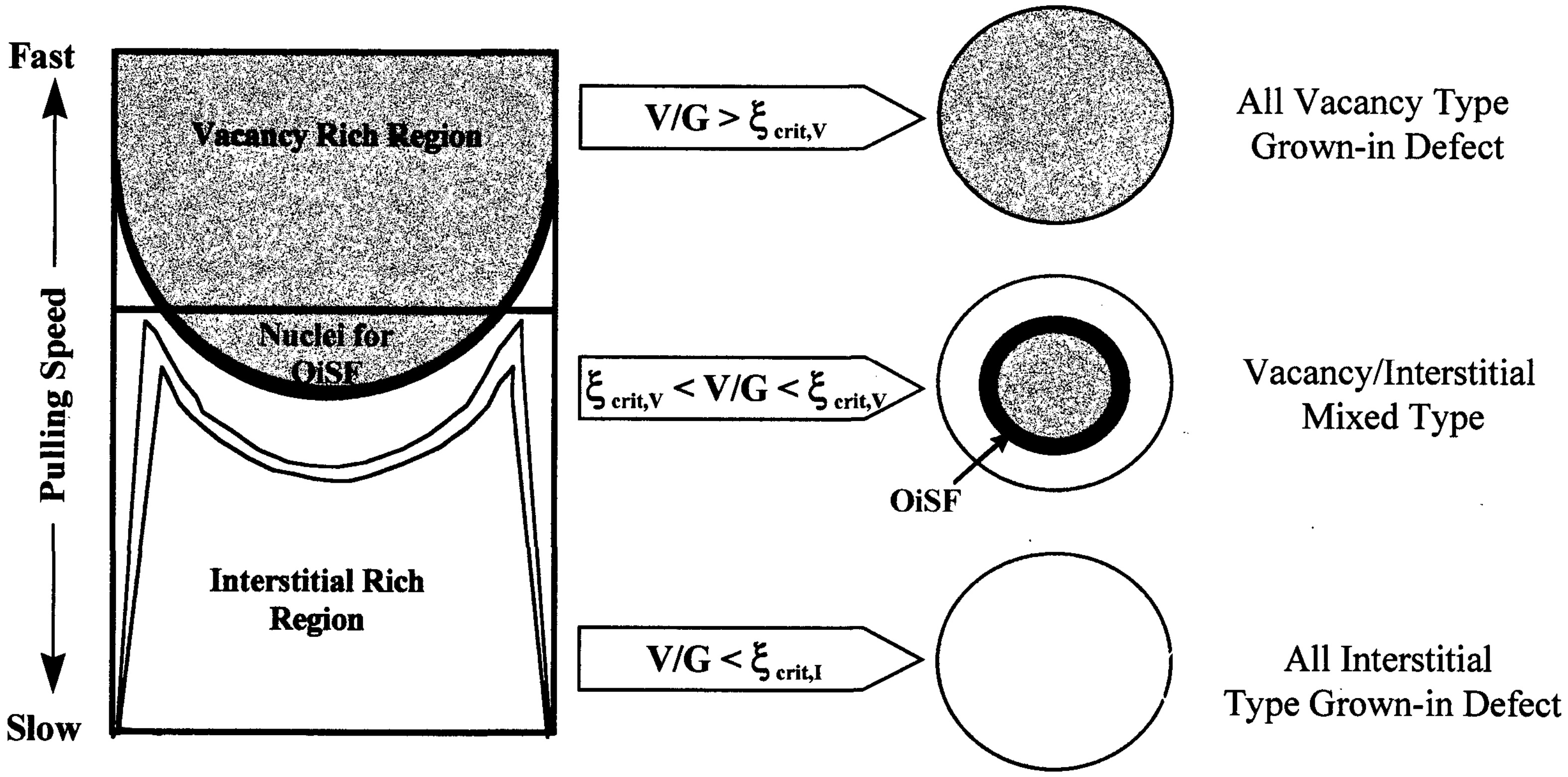

$V/G > \xi_{crit,V}$ → All Vacancy Type Grown-in Defect

$\xi_{crit,V} < V/G < \xi_{crit,V}$ → Vacancy/Interstitial Mixed Type

$V/G < \xi_{crit,I}$ → All Interstitial Type Grown-in Defect

V : Crystal Pulling Rate
G : Axial Temperature Gradient at Interface
ξ_{crit} : Critical Value

Crystal Quality of Fast Pulled Wafer

Uniformity of Oxygen Precipitates*

Normal Wafer

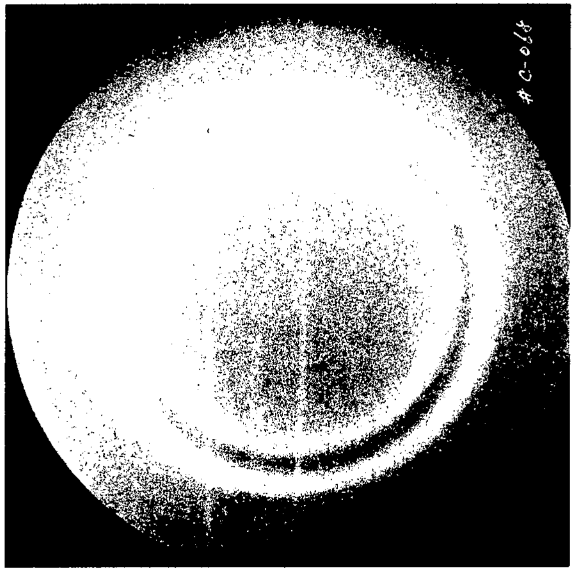

Fast Pulled Wafer

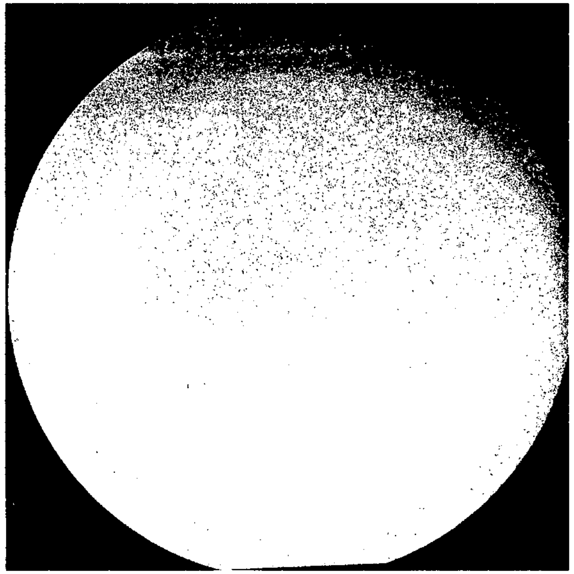

* Measured by x-ray topography after CMOS Simulation, (220) plane

Fast Pulling

Available Maximum Pull speed (conduction limited case)

$$K_s G_s = K_l G_l + V L$$

$$if\ K_l G_l = 0,\ V \Rightarrow V_{\max}$$

$$K_s G_s = V_{\max} L\ , \qquad \frac{V_{\max}}{G_s} = \frac{K_s}{L}$$

$$K_s = 22\ \mathrm{W/mK},\quad L = 4.19\ \mathrm{X}\ 10^9\ J/m^3$$

$$\therefore \frac{V_{\max}}{G_s} = 0.315\ (mm^2/\min K) \equiv \xi_{\max}$$

$$cf)\ \xi_{crit,V} = 0.138\ (mm^2/\min K)$$

$$in\ reality\ \ 0.138 < \xi_{\max} < 0.315$$

$$we\ conformed\ \ \xi_{\max} \cong 0.2\ (mm^2/\min K)$$

Available Maximum Pull speed (radiation limited case)

Billig's Expression

$$V_{\max} = \frac{\sqrt{2\,\sigma\,\varepsilon\,K_m T_m^5 / 3r}}{L\,\sigma_m} \quad \sim \text{Billig's expression, 1955}$$

K_m ~ Thermal conductivity of solid crystal at the melting temp.

σ_m ~ Density of the crystal at the melting Temp.

T_m ~ Melting temp. of the crystal

Assumptions

I) Heat loss from the crystal is only crystal by radiation.
ii) solid liquid interface is planer
iii)Thermal conductivity is temperature dependent
iv) emissivity is temperature independent

Available Maximum Pull Speed

Samuel's Result

$$\frac{d}{dx}\left(k\frac{dT}{dx}\right) - V\sigma c\frac{dT}{dx} - \frac{2h}{r}(T - T_a) - \frac{2}{r}q_r = 0$$

V: Pull speed
c : specific heat
h : thermal convective coeff.
T_a: average ambient temp.
q_R: radiadion heat

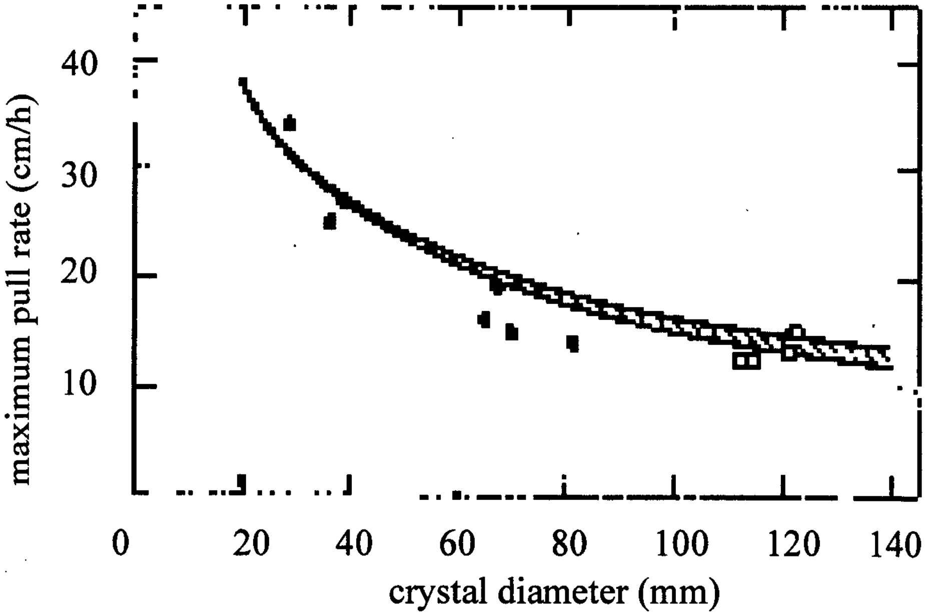

Fast Pulling

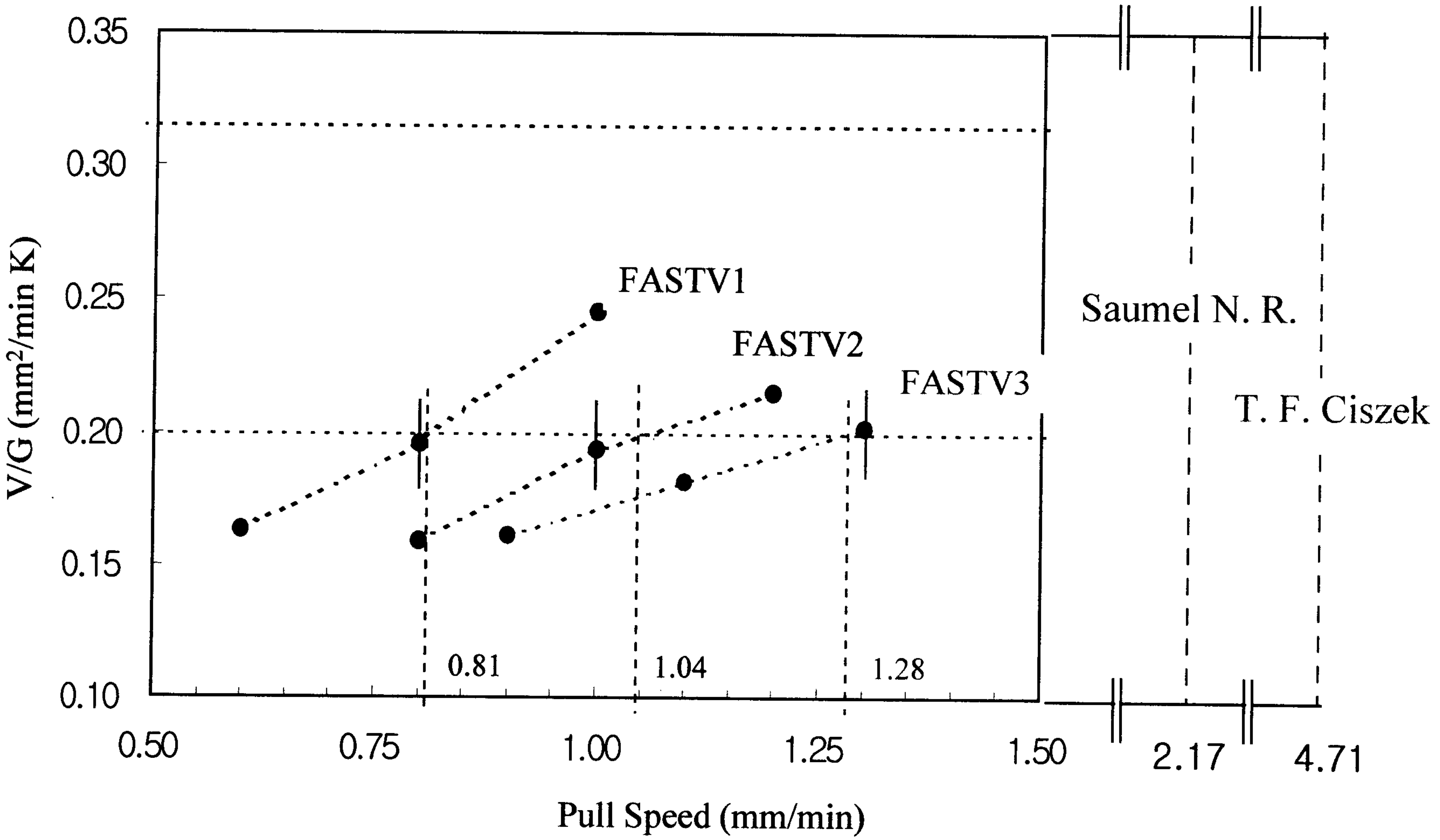

Conclusions (II)

- Axial temperature gradient G at the center of crystal/melt interface has been calculated using global simulator for growing Czochralski silicon crystal STHAMAS.

- It is known well that radial position of oxidation induced stakinf fault ring, which appears when $\xi_{crit} = V/G = 0.138\ mm^2/min\ K$.

- In other hand, Available maximum pull speed can be found when $0.138\ mm^2/\min K < V/G_{max} < 0.315 mm^2/\min K$, which is estimated for the conduction limit case.

- Experiment data was present available maximum pull speed appears when $V/G \cong 0.2\ mm^2/\min K$.